Modelling LAI, surface water and carbon fluxes at high-resolution over France: comparison of ISBA-A-gs and ORCHIDEE

S. Lafont, Y. Zhao, J. -C. Calvet, P. Peylin, Philippe Ciais, Fabienne Maignan, Marie Weiss

Biogeosciences, 9, 439–456, 2012
www.biogeosciences.net/9/439/2012/
doi:10.5194/bg-9-439-2012

Biogeosciences

Modelling LAI, surface water and carbon fluxes at high-resolution over France: comparison of ISBA-A-gs and ORCHIDEE

S. Lafont[1], Y. Zhao[2], J.-C. Calvet[1], P. Peylin[2], P. Ciais[2], F. Maignan[2], and M. Weiss[3]

[1]CNRM-GAME, Météo-France, CNRS, URA1357, Toulouse, France
[2]LSCE, Institut Pierre-Simon Laplace (IPSL), CEA-CNRS-UVS, UMR1572, Gif-sur-Yvette, France
[3]INRA, EMMAH, UMR1114, Avignon, France

Correspondence to: J.-C. Calvet (jean-christophe.calvet@meteo.fr)

Received: 7 July 2011 – Published in Biogeosciences Discuss.: 22 July 2011
Revised: 10 January 2012 – Accepted: 12 January 2012 – Published: 25 January 2012

Abstract. The Leaf Area Index (LAI) is a measure of the amount of photosynthetic leaves and governs the canopy conductance to water vapor and carbon dioxide. Four different estimates of LAI were compared over France: two LAI products derived from satellite remote sensing, and two LAI simulations derived from land surface modelling. The simulated LAI was produced by the ISBA-A-gs model and by the ORCHIDEE model (developed by CNRM-GAME and by IPSL, respectively), for the 1994–2007 period. The two models were driven by the same atmospheric variables and used the same land cover map (SAFRAN and ECOCLIMAP-II, respectively). The MODIS and CYCLOPES satellite LAI products were used. Both products were available from 2000 to 2007 and this relatively long period allowed to investigate the interannual and the seasonal variability of monthly LAI values. In particular the impact of the 2003 and 2005 droughts were analyzed. The two models presented contrasting results, with a difference of one month between the average leaf onset dates simulated by the two models, and a maximum interannual variability of LAI simulated at springtime by ORCHIDEE and at summertime by ISBA-A-gs. The comparison with the satellite LAI products showed that, in general, the seasonality was better represented by ORCHIDEE, while ISBA-A-gs tended to better represent the interannual variability, especially for grasslands. While the two models presented comparable values of net carbon fluxes, ORCHIDEE simulated much higher photosynthesis rates than ISBA-A-gs (+70 %), while providing lower transpiration estimates (−8 %).

1 Introduction

Terrestrial vegetation is an important component of the earth system. It has a strong impact on the exchange of energy, water and carbon between the land surface and the atmosphere. Vegetation controls the release in the atmosphere of the water stored in the soil and thus the partition between sensible and latent fluxes. Also, the plant-soil system controls the uptake and release of carbon dioxide from and to the atmosphere, through photosynthesis and respiration. In addition, the plant growth is governed by the climate. Improving the modelling of the land surface physiological processes is required to provide quantitative estimates of the surface fluxes for meteorological, hydrological and climate applications. Sensitivity and impact studies using state-of-the-art climate models have shown the importance of the vegetation-climate feedback (Dickinson et al., 1991; Garratt, 1993, Seneviratne et al., 2006). Continuous efforts were conducted to improve land surface model performances at various scales, especially concerning the modelling of the vegetation component (Brut et al., 2009). Indeed, a number of land surface models have evolved to include biogeochemical processes (Foley et al., 1996; Sellers et al., 1996; Calvet et al., 1998; Calvet and Soussana, 2001; Pitman, 2003; Krinner et al., 2005), and are able to simulate the surface energy, carbon and water fluxes, together with the vegetation biomass and the Leaf Area Index (LAI). The latter represents the one-sided green leaf area of vascular plants and is a key component of the canopy conductance to CO_2 and water vapour.

The model improvements have to be thoroughly tested in contrasting environmental and modelling conditions. This effort is needed, in order to reduce the uncertainty of model

results. For example, Jung et al. (2007) analyzed the Gross Primary Productivity (GPP) simulated by several Land Surface Models (LSM) over Europe, forced by different climate data and using several land cover types. They showed that the differences between the models were the most important factors affecting the simulation of GPP. Differences in climate forcing and land cover types came second and third, respectively.

There are various ways of evaluating LSMs. They can be compared at the site level, forced by atmospheric measurements in a data-rich context. For example, the FLUXNET sites (Baldocchi et al., 2008) form a network of in situ measurements that provide a quasi-continuous monitoring of energy, water and carbon fluxes based on eddy covariance devices. Up to now, using local in situ observations was a common benchmarking procedure because the abundance of data allows to better constrain the models. Such intercomparisons are a very powerful tool to evaluate the models at a local scale (Viovy, 2003; Morales et al., 2005; Gibelin et al., 2008).

However, using local in situ observations is not sufficient. A correct representation of the processes at a local scale does not ensure a correct representation at larger spatial scales. In order to validate LSMs from the landscape scale to the global scale, large-scale datasets are needed. Remotely sensed data are thus very valuable to provide continuous and coherent spatial information over large domains.

In recent years, a lot of efforts were dedicated to use Earth observation satellite information to derive key biophysical parameters, including LAI (Baret et al., 2007; Weiss et al., 2007; Garrigues et al., 2008). In order to use this information into LSMs, data assimilation techniques were implemented and tested (Demarty et al., 2007; Sabater et al., 2008; Albergel et al., 2010a; Barbu et al., 2011). Data assimilation techniques aim at improving the model simulations, which are affected by uncertainties, mainly caused by the lack of knowledge of some biophysical processes, together with errors in the atmospheric variables used as input to the models (Szczypta et al., 2011; Zhao et al., 2011). A first step before implementing data assimilation techniques is to perform an error analysis of both model simulations and satellite products.

The comparison of LAI estimates with in situ measurements is needed to evaluate both LAI simulations and remote sensing products (Calvet et al., 1998; Ganguly et al., 2008; Garrigues et al., 2008). However, due to the limited number of sites observing this variable, the representativeness of local observations is limited. Therefore, it is useful to compare the spatial distribution of LAI at larger scales. The extrapolation at the landscape scale of the results obtained at the site scale is not trivial, in part because there is usually less information available to characterise the surface (initial conditions, model parameters).

In this study, the two French land surface models ORCHIDEE (Krinner et al., 2005) and ISBA-A-gs (Calvet et al., 1998, 2000, 2004) are used. In previous works (Viovy, 2003; Gibelin et al., 2008), the carbon, water and energy fluxes simulated by the two models were compared at the site scale for several vegetation types and, overall, similar scores were obtained. This study aims at extending the intercomparison of the two models at the landscape scale. The France domain is considered, with a relatively high spatial resolution of 8 km, and remote sensing data are used to provide continuous and consistent spatial information over the domain. A careful set-up of the simulations for both models ensures that the observed differences are primarily related to differences in model parameterisation. The seasonal cycle and the interannual variability of the LAI simulated by the models are investigated by comparing them with two remote sensing products. Also, the carbon and water fluxes simulated by the two models are compared, in terms of seasonal cycle, interannual variability, in relation to the most frequent Plant Functional Types (PFT) in France. This study complements the evaluation of the ISBA-A-gs model performed by Brut et al. (2009) over southwestern France, as it is expanded to the whole of France. Moreover, a longer time period is considered and the analysis includes the ORCHIDEE model. In Sect. 2, the atmospheric and land cover data used to force the model simulations are described, together with the two models used in this study. The results are presented in Sect. 3, including an analysis of the differences between the two models in terms of LAI seasonality, interannual variability (in particular, the impact of the 2003 and 2005 droughts), and of the carbon and water fluxes. The analysis is performed both at the 8 km × 8 km grid-cell scale, and for each PFT. The results are discussed in Sect. 4, and the main conclusions of this study are summarized in Sect. 5.

2 Data and models

2.1 The ECOCLIMAP-II parameter map

The ECOCLIMAP database (Masson et al., 2003) provides detailed information about the land cover at a global scale, with a spatial resolution of 1 km. In this study, a new version of the ECOCLIMAP dataset (Faroux et al., 2009) was used. It contains an updated classification of vegetation types over Europe and North Africa. The ECOCLIMAP-II dataset includes 257 classes and provides rules to aggregate these ecosystems into 12 PFTs. Over the France domain, the main ECOCLIMAP-II PFTs are grasslands (31 %), C3 crops (24 %), broadleaf forests (20 %), coniferous forests (11 %), bare soil (8 %), C4 crops (4 %). Note that the main difference between ECOCLIMAP-II and the previous version is a marked decrease of the fraction of C3 crops and an increase of the fraction of grasslands (40 % and 21 % in the previous version, respectively). The same ECOCLIMAP-II PFT fraction map was used by the two LSMs ORCHIDEE and ISBA-A-gs (Sect. 2.4).

2.2 Meteorological forcing: the SAFRAN analysis

The main objective of the "Système d'Analyse Fournissant des Renseignements A la Neige" (SAFRAN) analysis is to produce an accurate estimation of the atmospheric variables needed by LSMs over France (Quintana-Segui et al., 2008). SAFRAN uses an optimal interpolation method to analyze surface atmospheric variables (Durand et al., 1993, 1999). One of the main features of SAFRAN is that the analyses are performed over climatologically homogeneous zones, which are areas of irregular shape and cover a surface usually smaller than 1000 km^2 and where the horizontal climatic gradients are weak. SAFRAN estimates one value of each variable for each zone at several altitude levels.

As input, SAFRAN uses observations from the automatic, synoptic and climatological networks of Météo-France and a first guess from large scale operational weather prediction models. In particular, information from more than 1000 meteorological stations and more than 3500 daily rain gauges throughout France is used. First, SAFRAN performs a quality control of the observations. This is an iterative procedure based on the comparison between observed and analyzed quantities at the observation location. The analyses of air temperature, air humidity, wind speed, and cloudiness are performed every 6 h using all the available observations. For these variables, the first guess comes from the large-scale operational weather prediction model ARPEGE (Courtier et al., 1991) or from the ECMWF operational archives. Next, the analysed values are interpolated to an hourly time step. All altitude profiles (air temperature, air humidity, and cloudiness), and surface wind, are linearly interpolated. Also, the incoming solar radiation and the incoming longwave radiation (ISR and ILR, respectively) are calculated using a radiative transfer scheme (Ritter and Geleyn, 1992), which uses the vertical profiles previously calculated. The spatial resolution of the analyses used in this study corresponds to a 8 km $\times$ 8 km grid.

Vidal et al. (2010) noticed a lack of input observations to the radiation transfer scheme in some regions (e.g. the southern part of Massif Central), which leads to an overestimation of ISR and to an underestimation of ILR. Coastal areas present some biases too. SAFRAN also appears to underestimate the daily maximum of ISR (Quintana-Segui et al., 2008). On average, the cumulated ISR is underestimated by 5 % (Szczypta et al., 2011).

2.3 Satellite-derived LAI products

2.3.1 The CYCLOPES SPOT/VGT product

The CYCLOPES project was an initiative aiming at developing and producing global surface parameters from spaceborne sensors. In particular, key biophysical parameters (LAI, fAPAR and fCover) were produced for the period 1998–2007 based on the processing of SPOT/VEGETATION data (Baret et al., 2007). Top of canopy reflectance values were corrected for surface directional effects in order to obtain normalized reflectances. A neural network was used to retrieve LAI from the normalized reflectances. The neural network was previously trained from synthetic reflectances produced by the SAIL model (Verhoef, 1984) simulating the radiation transfer within vegetation canopies. In this study, the Version 3.1 of the CYCLOPES LAI product (Postel, 2008; http://postel.mediasfrance.org) is used. It has a spatial resolution of 1 km and a 10-day temporal frequency, with a narrow Gaussian filter (Baret et al., 2007) based on a temporal composite window of 30 days ($\pm$15 days). The 30-d composite window is centred on the date of interest. It is used to smooth the LAI signal in case of missing dates, caused for example by the presence of clouds. The accuracy of this product was investigated by Weiss et al. (2007) and CYCLOPES was found to present a good agreement with in-situ measurement, with maximum LAI values lower than other products. Also, Weiss et al. (2007) have shown that the temporal profile of the CYCLOPES LAI presents the same timing than the MODIS product. It must be noted that CYCLOPES provides effective LAI values, which are generally lower than true LAI estimates accounting for the vegetation clumping (Chen et al., 2005).

2.3.2 The MODIS collection 5 product

The MODIS LAI retrieval algorithm relies on a stochastic radiative transfer model (Knyazikhin et al., 1998) which ingests red and infrared reflectance values, their uncertainties, and the view-illumination geometry. The algorithm uses the MODIS land cover (MOD12Q1) product (Friedl et al., 2002) as a priori information to constrain the LAI outputs. A look-up table compares observed and modelled reflectances for a suite of canopy structures and soil patterns that represents an expected range of typical conditions for a given biome type. The daily LAI is retrieved as the mean value from all possible solutions within a specific level of input satellite data and model uncertainties. The products have a spatial resolution of 1km and a 8-day temporal frequency. If this algorithm fails, a back-up procedure is triggered to estimate LAI from biome specific NDVI based relationships. In this study, the Collection 5 version of the MODIS LAI product was used. Conversely to CYLOPES, the MODIS LAI partly accounts for the vegetation clumping. The accuracy of the MODIS collection 5 LAI was evaluated by Ganguly et al. (2008). Inter-comparison exercises between CYCLOPES and MODIS LAI were also conducted (Garrigues et al., 2008; Verger et al., 2009).

2.4 The land surface models

2.4.1 The ORCHIDEE model

ORCHIDEE (Krinner et al., 2005) is a process-based terrestrial biosphere model designed to simulate ecosystem, energy, water, and carbon fluxes at half-hourly to decadal time scales. ORCHIDEE contains three sub-modules, a land surface energy and water balance model SECHIBA (De Rosnay and Polcher, 1998), a land carbon cycle model STOMATE, and a dynamic model of long-term vegetation dynamics including competition and disturbances adapted from LPJ (Sitch et al., 2003). In this study, the spatial distribution of vegetation types is prescribed, based on ECOCLIMAP-II. The spatial heterogeneity of the vegetation is described through 13 PFTs, of which five are relevant for this study (temperate broadleaf forests, temperate coniferous forests, grasslands, C3 crops and C4 crops). The instantaneous energy and water balance of vegetated and non-vegetated surfaces is simulated, as well as the canopy-level photosynthesis, using coupled leaf-level photosynthesis and stomatal conductance processes (Ball et al., 1987; Farquhar et al., 1980). Stomatal conductance is reduced by soil water stress (McMurtrie et al., 1990), as a function of soil moisture and root profiles. Two soil water reservoirs are considered, a surface reservoir which refills in response to rain events and which is brought to zero during dry periods, and a deeper soil reservoir considered as a simple bucket updated accounting for evaporation, root uptake, percolation and runoff. ORCHIDEE uses a tiled approach (allowing the simulation of different PFTs within a grid cell), and the tiles of a grid cell share the same soil water reservoir. The version of ORCHIDEE used in this study includes a new phenology module for two PFTs: C3 crops and grasslands (Maignan et al., 2011). The soil carbon cycle of the model is put in equilibrium with a long spin-up procedure (of more than 500 yr).

2.4.2 The ISBA-A-gs model within SURFEX

Météo-France has developed the SURFEX platform (SURFace EXternalisée) to be used in operational NWP models, and offline for applications in hydrology and vegetation monitoring (Le Moigne et al., 2009). Over land, SURFEX includes ISBA-A-gs, a CO_2-responsive LSM (Calvet et al., 1998, 2004; Gibelin et al., 2006; Calvet et al., 2008) able to simulate the diurnal cycle of carbon and water vapour fluxes, together with LAI and soil moisture. This model accounts for different feedbacks in response to long-term changes in atmospheric concentration of CO_2, and provides a representation of photosynthesis enhancement and transpiration reduction (fertilization and reduced transpiration effects, respectively). The model also includes an original representation of the soil moisture stress. Two different types of drought responses are distinguished for both herbaceous vegetation (Calvet, 2000) and forests (Calvet et al., 2004), depending on the evolution of the water use efficiency (WUE) under moderate stress: WUE increases in the early soil water stress stages in the case of the drought-avoiding response, whereas WUE decreases or remains stable in the case of the drought-tolerant response. ISBA-A-gs calculates interactively the leaf biomass and the LAI, using a simple growth model (Calvet et al., 1998). Gibelin et al. (2006) and Brut et al. (2009) showed that ISBA-A-gs provides reasonable LAI values at regional and global scale under various environmental conditions. The ecosystem respiration (Reco) is described in the model as a basal rate modulated as a function of soil moisture and soil temperature (Albergel et al., 2010b). In this study, the basal rates were calibrated to obtain an equilibrium between Reco and the vegetation carbon uptake over the length of the simulation.

2.4.3 Main differences between ISBA-A-gs and ORCHIDEE

The two models used in this study share the same general structure, allowing the description of the same biophysical processes. However, they have been developed independently, and the way the processes are represented can differ greatly. Those relevant to this study include the photosynthesis module and the phenology (see below). Also note that other processes may impact photosynthesis and the vegetation biomass, such as the representation of the soil hydrology, the surface albedo, the resolution of the surface energy budget, etc.

ISBA-A-gs uses a CO_2 responsive parameterization of photosynthesis based on the model of Goudriaan et al. (1985) modified by Jacobs (1994) and Jacobs et al. (1996). This parameterization is derived from the set of equations used in ORCHIDEE (Farquhar et al., 1980 for C3 plants and Collatz et al., 1992 for C4 plants), and it has the same formulation for C4 plants as for C3 plants, differing only by the input parameters. Moreover, the slope of the response curve of the light-saturated net rate of CO_2 assimilation to the internal CO_2 concentration is represented by the mesophyll conductance (g_m). Therefore, the value of the g_m parameter is related to the activity of the Rubisco enzyme (Jacobs et al., 1996), while in the Farquhar model, this quantity is represented by a maximum carboxylation rate parameter ($V_{c,max}$). The model also includes a detailed representation of the soil moisture stress (see Sect. 2.4.2).

ORCHIDEE has an explicit phenology model which computes leaf onset and leaf offset dates. This phenology submodel was calibrated globally using remote sensing data (Botta et al., 2000). For deciduous forests, the leaf onset is controlled by air temperature, only, while a dual constraint on soil moisture availability and air temperature is used for grasslands and crops. The temperature dependence is based on temperature sums, in units of Growing Degree Days and of Chilling Days. The senescence model is based on two criteria. First, the leaf turnover rate increases sharply when the

mean leaf age exceeds a maximum leaf age. Second, environmental conditions are accounted for, using air temperature for the forest PFT and air temperature and soil moisture availability for grasslands. Maignan et al. (2011) have recently improved the ORCHIDEE phenology model for crops, using specific parameter values for crops instead of using the same parameters for crops and for grasslands. A typical seasonal cycle simulated by ORCHIDEE presents (1) a dormancy phase, (2) a sharp increase of LAI over a few days at the leaf onset, (3) a more gradual growth governed by photosynthesis, until a maximum LAI value has been reached, (4) stable maximum LAI values until the senescence date has been reached, (5) a senescence phase presenting an exponential decline of LAI. The ISBA-A-gs growth model currently used in the SURFEX modelling platform (http://www.cnrm.meteo.fr/surfex/) is described in Gibelin et al. (2006). No specific phenology model is used, as the vegetation growth and senescence are entirely driven by photosynthesis. However, the LAI values are maintained above a minimum LAI threshold ($1\,m^2\,m^{-2}$ for coniferous forest, $0.3\,m^2\,m^{-2}$ for other PFTs). At wintertime, such low values may be reached, and prescribing minimum LAI values allows plant growth to start as soon as photosynthesis exceeds leaf respiration (i.e. net assimilation of CO_2 is positive). The leaf biomass turnover increases when the ratio of the actual photosynthesis to the maximum photosynthesis decreases. This usually triggers a decrease of LAI corresponding to the senescence. A typical seasonal cycle of LAI simulated by ISBA-A-gs starts with LAI at its minimum value. At springtime, LAI gradually increases, in relation with the rise in net assimilation values and with lower turnover rates. At summertime, when the soil moisture stress increases, the leaf biomass mortality tends, first, to counterbalance net assimilation and LAI reaches a maximum value or a plateau (at a value which is not predefined and which may vary from one year to another). In more marked summer drought conditions, the leaf biomass mortality exceeds net assimilation and LAI declines, down to the minimum value. Compared with the ORCHIDEE model simulation, the ISBA-A-gs LAI is more continuous, with a smoother evolution.

In this study, ISBA-A-gs uses the PFT-dependent parameters provided by ECOCLIMAP-II and described in Brut et al. (2009), while ORCHIDEE uses its default parameters.

ISBA-A-gs has nine main parameters listed in Brut et al. (2009) for various PFTs. The photosynthesis model is governed by four key parameters: the mesophyll conductance in well-watered conditions (g_m), the cuticular conductance, the critical extractable soil moisture content, and the response to drought (drought-avoiding or drought-tolerant). Plant growth is characterized by five parameters: the maximum leaf span time, the minimum leaf area index, the leaf nitrogen concentration N_L, the SLA (specific leaf area) sensitivity to N_L, and SLA at $N_L = 0\,\%$.

The PFT-dependent parameters of ORCHIDEE are detailed in Krinner et al. (2005) and in Le Maire et al. (2010). The main photosynthesis parameter is $V_{c,max}$, and the computation of stomatal conductance uses the parameters (slope and intercept) of Ball et al. (1987). The phenology model uses nine parameters: the mean leaf span time, the maximum LAI beyond which there is no allocation of biomass to leaves, the SLA, a daily temperature threshold for summing cumulated degree days, three parameters to compute the threshold cumulative degree day for leaf onset, a weekly temperature below which leaves are shed if seasonal temperature trend is negative, a weekly moisture stress below which leaves are shed.

2.5 Comparison of the various data sets

The two satellite-derived LAI products were re-projected on the 8km resolution grid of SAFRAN, and the two sets of model simulations were produced for the same grid (8602 grid cells). A quality check was performed for the MODIS product in order to sort out LAI values produced by the back-up algorithm. All the LAI values were averaged on a monthly basis. The common period for the two satellite data sets covered the years 2000 to 2007. The ORCHIDEE and ISBA-A-gs simulations covered the 1994–2007 period and monthly mean values were analysed. The same land cover map (ECOCLIMAP-II) and the same atmospheric forcing (SAFRAN) were used by the two models.

The model sub-grid variability is represented by individual simulations performed for each PFT present in the grid cell. The grid-cell simulated LAI is the average of the PFT-dependent LAI multiplied by the area covered by each PFT. As the reprojected satellite data consist of one value per grid cell, the analysis of the model performance for a given PFT was made for grid cells including a sufficient cover fraction of the considered PFT. The majority criterion was not used, as in many heterogeneous grid cells, the dominant PFT could have a relatively low cover fraction. The grid cells complying with the following criteria were selected:

- fractional cover of the dominant PFT above 0.25;
- fractional cover of the dominant type at least 0.10 higher than the fractional cover of the second most important PFT;
- average grid-cell elevation below 1200 m (in order to screen out permanent-snow areas).

The response of the four LAI products to the 2003 and 2005 droughts was investigated. The estimation of LAI may differ a lot from one product to another, both in terms of seasonal cycle and in terms of interannual variability. In order to better capture the response to the 2003 and 2005 droughts, and the differences from one product to another, scaled LAI anomalies were considered, rather than the original values.

The scaled anomalies where computed according to the equation:

$$\mathrm{Ano}(\mathrm{mo},\mathrm{yr}) = \frac{\mathrm{LAI}(\mathrm{mo},\mathrm{yr}) - \mathrm{avg}(\mathrm{LAI}(\mathrm{mo},:))}{\mathrm{stdev}(\mathrm{LAI}(\mathrm{mo},:))} \quad (1)$$

Where Ano(mo,yr) and LAI(mo,yr) are, respectively, the anomaly and the LAI for the month mo and the year yr; avg(LAI(mo,:)) and stdev(LAI(mo,:)) are the average and the standard deviation of the LAI of the month mo, for all years, respectively. For example a value of -1 of the scaled anomaly means than the LAI value is one standard deviation lower than the 2000–2007 climatology.

In order to suppress spatial differences in annual minimum and maximum climatologic LAI values, scaled LAI values, ranging between 0 and 1 for each grid cell, were produced, also.

3 Results

3.1 Comparison of the four LAI estimates

The period of eight years (2000–2007) for which LAI remote sensing data were available was selected. Figure 1 presents the average monthly evolution of LAI over France for the two models and for the two remote sensing products. The left panel represents the actual LAI values, whereas the right panel represents the scaled LAI values. The first striking feature is that the two models present higher maximum values than the remote sensing products. Also, the start of the growing season is earlier in the ORCHIDEE simulation. ISBA-A-gs presents a leaf onset lag of about one month with respect to ORCHIDEE (as shown by the similarity of the April LAI simulated by ORCHIDEE and the May LAI simulated by ISBA-A-gs). The main difference between the modelled and the satellite-derived LAI is observed for the Massif Central grasslands in April. While many simulated values are still lower than $1\,\mathrm{m^2\,m^{-2}}$, most satellite-derived values are higher than $2\,\mathrm{m^2\,m^{-2}}$, especially for MODIS. A few independent in situ LAI observations were presented by Vuichard et al. (2007). They reported low LAI values at springtime ($1\,\mathrm{m^2\,m^{-2}}$ or less) followed by a rapid rise in June, up to $2.5\,\mathrm{m^2\,m^{-2}}$. There are marked differences between the two remote sensing products. In March, the MODIS product presents maximum values over the Massif Central grassland, whereas in July, it presents very low values over the crop area of northern France.

The right panel of Fig. 1 presents scaled LAI value. This allows a better comparison of the timing of the phenological cycle. In particular, the two satellite scaled LAI maps present an excellent agreement. On the other hand, the differences in leaf onset and leaf offset, between the two models, and between the models and the satellite products are still clearly visible. In spring, the start of the growing season presents smoother patterns in the models than in the satellite products. The smoother model patterns are related to air temperature with higher scaled LAI values along coastal areas and lower values in northeastern France and in mountainous areas. The satellite products present more fine scale variability, with high values in western and central France. In July and August, MODIS and CYCLOPES present a marked decline of the scaled LAI in the northern half of France (blue colour) with a marked east-west limit. During this period, the two models show a decrease in scaled LAI, also, in the western part of the domain, but with a southwest-northeast limit. Despite the temporal shift between the models, they present rather similar spatial patterns at summertime, especially at the boundary between senescent and growing areas. From this point of view, both models differ from the satellite products. The similarity of the two models suggest that this difference comes from the model input data sets, either the land cover map or the SAFRAN atmospheric forcing.

The LAI has a strong seasonal cycle, and this implies that the temporal correlation between two time series of LAI is very sensitive to any shift in the seasonal cycle. For instance the correlation of the CYCLOPES product with itself, lagged by one month, is on average $r = 0.7$. In order to investigate this issue, the temporal correlation of the monthly products was computed for each pair of product, for each grid cell. The correlation of the simulated LAI series with the CYCLOPES time series of LAI was calculated for each point (Fig. 2, middle column). Overall ORCHIDEE presents higher correlations with most values above 0.8 with the exception of the western part of the domain. ISBA-A-gs presents higher correlations over southern France than in northern France. In order to assess differences in leaf onset, a one-month lag was subtracted to the model time series (this assumes a leaf onset one month earlier), and the correlation was computed again (Fig. 2, right column). The correlation significantly increases for the ISBA-A-gs simulations over most of France, showing that the model tends to simulate a delayed seasonal cycle. On the other hand, the correlations for the ORCHIDEE simulation tend to decrease. When a one-month lag is added (this assumes a leaf onset simulated one month later), the correlation for the ORCHIDEE simulation can be locally improved in the north of France and over the Les Landes forest (Fig. 2, left column). This lag has only a negative impact on the ISBA-A-gs simulations. Using the MODIS LAI product instead of the CYCLOPES data (not shown) leads to similar conclusions.

The spatial correlation of monthly averaged LAI values, from one product to another (Table 1), presents a marked seasonal cycle. In winter and spring, only the models have a strong spatial correlation, while the correlation between models and satellite products is very low (r^2 below 0.25) regardless of the model or of the satellite product. These low values can be explained by the lack of spatial feature in the LAI maps, associated to disagreements between models and satellite products for low LAI values. The spatial correlation in summer (JAS) is around $r^2 = 0.5$ for all combinations (except for ISBA-A-gs vs. MODIS, presenting the

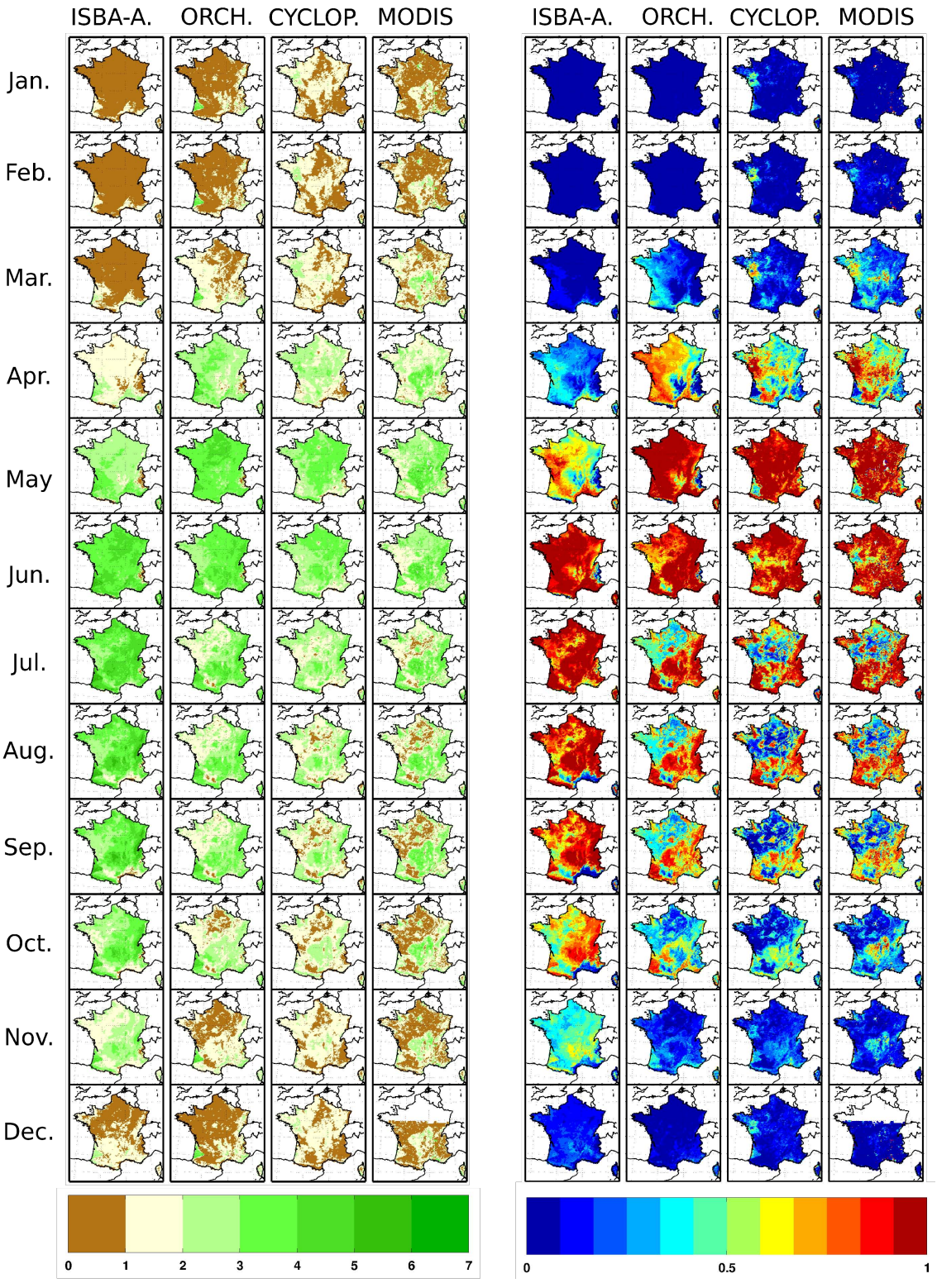

Fig. 1. Monthly climatology (2000–2007) over France of (left) LAI and (right) scaled LAI. Each subfigure presents, (from left to right) the two models ISBA-A-gs and ORCHIDEE, the two remote sensing products, CYCLOPES, and MODIS, and (from top to bottom) January to December. Note that the MODIS product is not available in northern France in December because of a threshold in the main MODIS algorithm for the zenith solar angle.

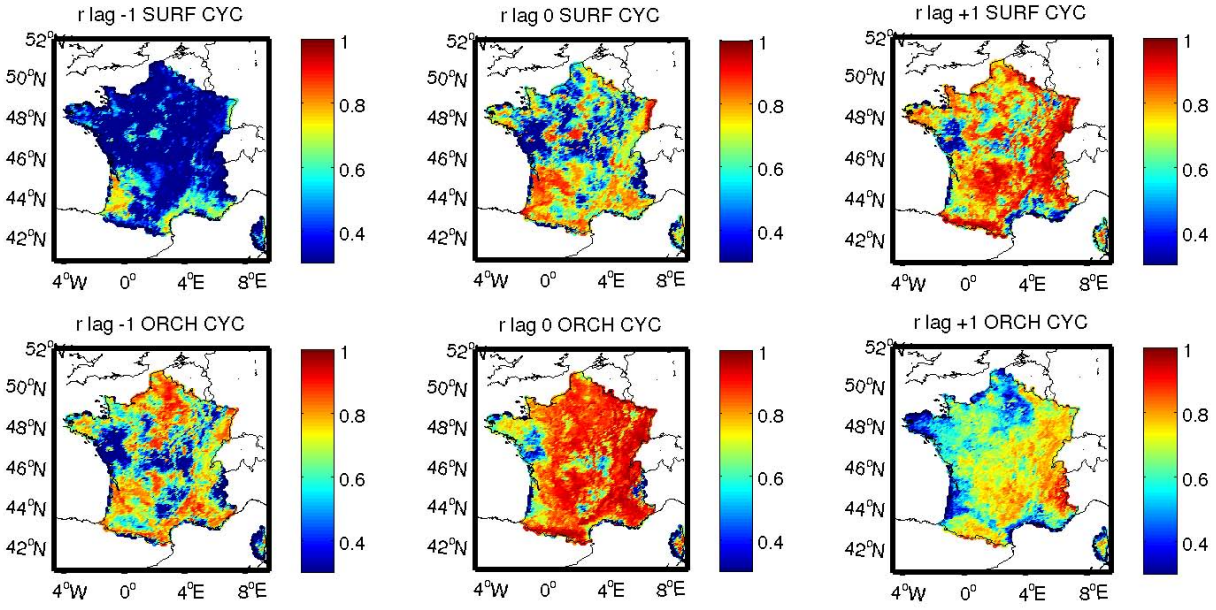

Fig. 2. Lagged and unlagged temporal correlation of monthly LAI values for the 2000–2007 period of the CYCLOPES remote sensing product with (top) ISBA-A-gs and (bottom) ORCHIDEE. Three lags of the models with respect to CYCLOPES are considered (from left to right): models advanced by one month, no lag, models delayed by one month.

Table 1. Spatial correlation (r^2) of the average monthly LAI (2000–2007) per season and for all the possible combination of the ORCHIDEE and ISBA-A-gs models (ORC, ISBA, respectively) and remote sensing (RS) CYCLOPES and MODIS products (CYC, MOD, respectively). From left to right: model vs. RS, model vs. model, RS vs. RS comparisons. For each 3-month period, the spatial correlations are calculated using the three pooled monthly maps.

r^2	ORC/CYC	ORC/MOD	ISBA/CYC	ISBA/MOD	ISBA/ORC	CYC/MOD
JFM	0.00	0.07	0.00	0.09	0.58	0.13
AMJ	0.25	0.09	0.12	0.07	0.37	0.21
JAS	0.51	0.58	0.53	0.36	0.46	0.58
OND	0.17	0.22	0.25	0.18	0.43	0.43

lowest value). For all the seasons, the spatial correlation between models never falls below 0.37, which can be partially explained by the use of a common land cover map. The correlation between CYCLOPES and MODIS products is higher in summer and during the autumn (r^2 ranges from 0.43 to 0.58) than in winter and spring (below 0.3). Using scaled LAI maps (Fig. 1, right panel) markedly improves the latter scores at summertime, with r^2 reaching 0.74.

3.2 Interannual variability of LAI

The interannual variability, expressed as the monthly coefficient of variation (CV, the ratio of the standard deviation divided by the mean value), differs a lot from one LAI source to another (Fig. 3). The highest values of CV (above 70 %) are reached over northern France in March for the ORCHIDEE model, in relation to a high variability and low average values. The lowest values (about 10 % on average) are obtained in July, with ORCHIDEE, also. The ISBA-A-gs model, on the other hand, has a larger variability at the end of the growing season (August and September). The satellite products tend to have a lower variability (CV below 30 %), with the highest values observed in autumn and at wintertime.

In order to investigate further the ability of the models to represent the interannual variation of LAI vs. the satellite products, the average and standard deviation of the grid cell correlation coefficients (r) of the monthly LAI time series and of the monthly LAI anomalies are displayed in Fig. 4, for each PFT. The LAI anomaly consist in the deviation to the mean, computed by substracting the average seasonal cycle from the LAI time series. The interannual variation of LAI for a given month is a much smaller signal that the year-round seasonal cycle, leading to lower r values of the former, with r generally below 0.5, except for grasslands simulated by ISBA-A-gs. Apart from the broadleaf forests, ISBA-A-gs

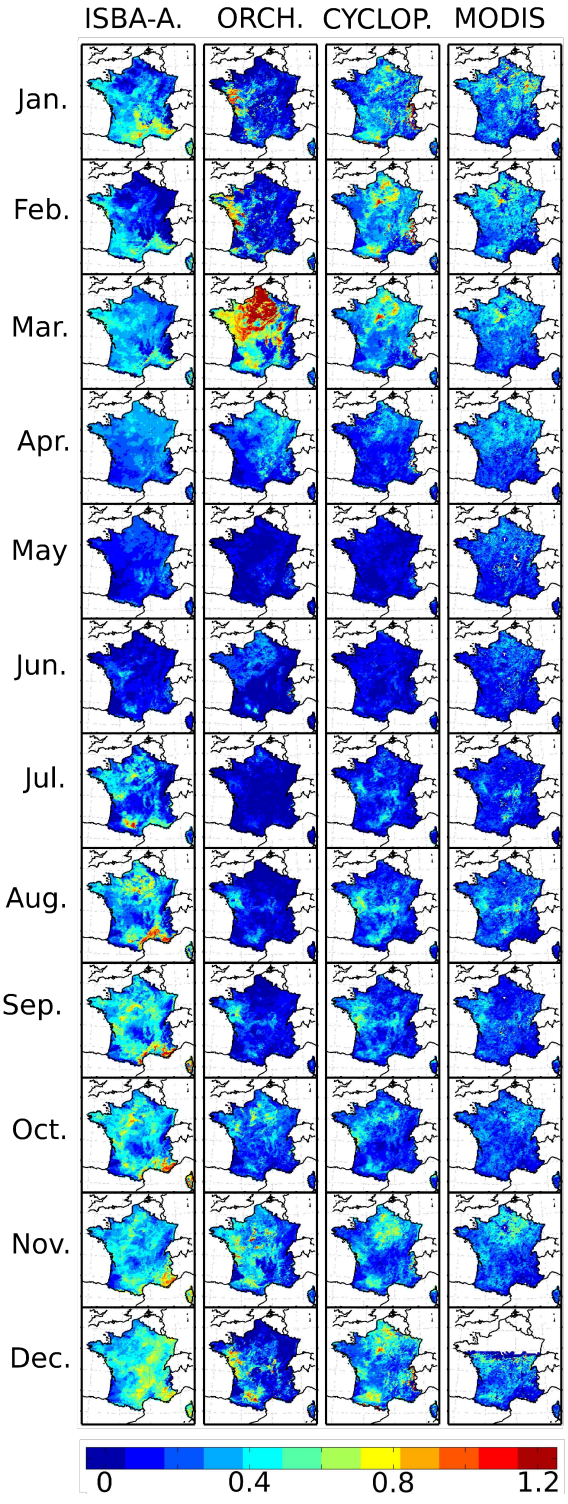

Fig. 3. Monthly LAI interannual variation (coefficient of variation) of (from left to right) ISBA-A-gs and ORCHIDEE models, and CYCLOPES and MODIS remote sensing products.

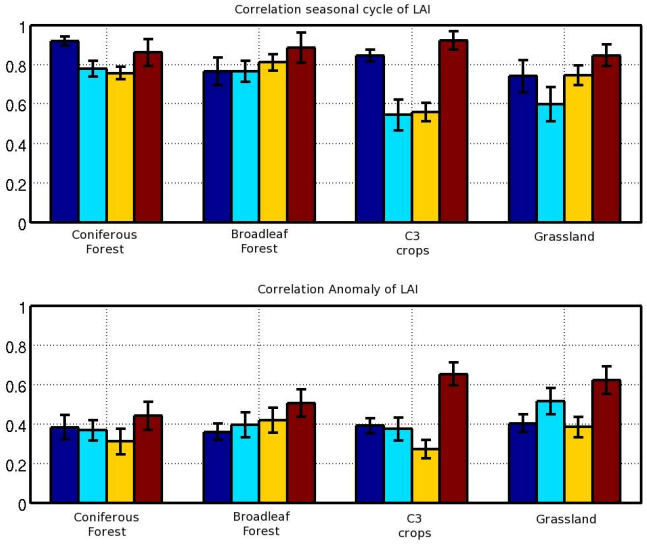

Fig. 4. Average temporal correlation (r) over France of (top) monthly LAI time series and (bottom) monthly time series of LAI anomalies, and standard deviation (bars), per Plant Fonctional Type. Dark blue: ORCHIDEE vs. CYCLOPES; light blue: ISBA-A-gs vs. CYCLOPES; yellow: ORCHIDEE vs. ISBA-A-gs; brown: CYCLOPES vs. MODIS.

correlates less than ORCHIDEE with the CYCLOPES seasonal cycle, consistent with the discrepancy in leaf onset observed in Fig. 2. The difference in r is particularly marked for C3 crops. On the other hand, the ISBA-A-gs LAI anomalies present r values similar to the ORCHIDEE r values, or higher in the case of grasslands. This is an indication that the marked summertime interannual variability of ISBA-A-gs (Fig. 3) is consistent with CYCLOPES, especially for grasslands.

3.3 Impact of the droughts of 2003 and 2005

Figure 5 presents the evolution of the scaled anomaly Eq. (1), in 2003 and in 2005, for the four LAI products. In May 2003, the LAI simulated by the two models is higher than the 2000–2007 average value (positive anomaly, in green), in response to above-average air temperatures. The two satellite products show a more contrasted pattern of positive and negative areas. In June 2003, the CYCLOPES product, and to a lesser extent the MODIS product, show contrasted spatial patterns, with above-normal LAI in northwestern France and a below-normal LAI in southeastern France. ISBA-A-gs shows a similar pattern, whereas ORCHIDEE presents a more uniform decrease of LAI. In July and August, the spatial agreement between model and satellite product anomalies is quite good, with spatial correlation coefficients higher than 0.5, with a rather consistent decline of LAI over the whole domain, from July to August. In September 2003, some regions in the MODIS product and in the ORCHIDEE model start showing a positive anomaly. In October, the remote sensing products

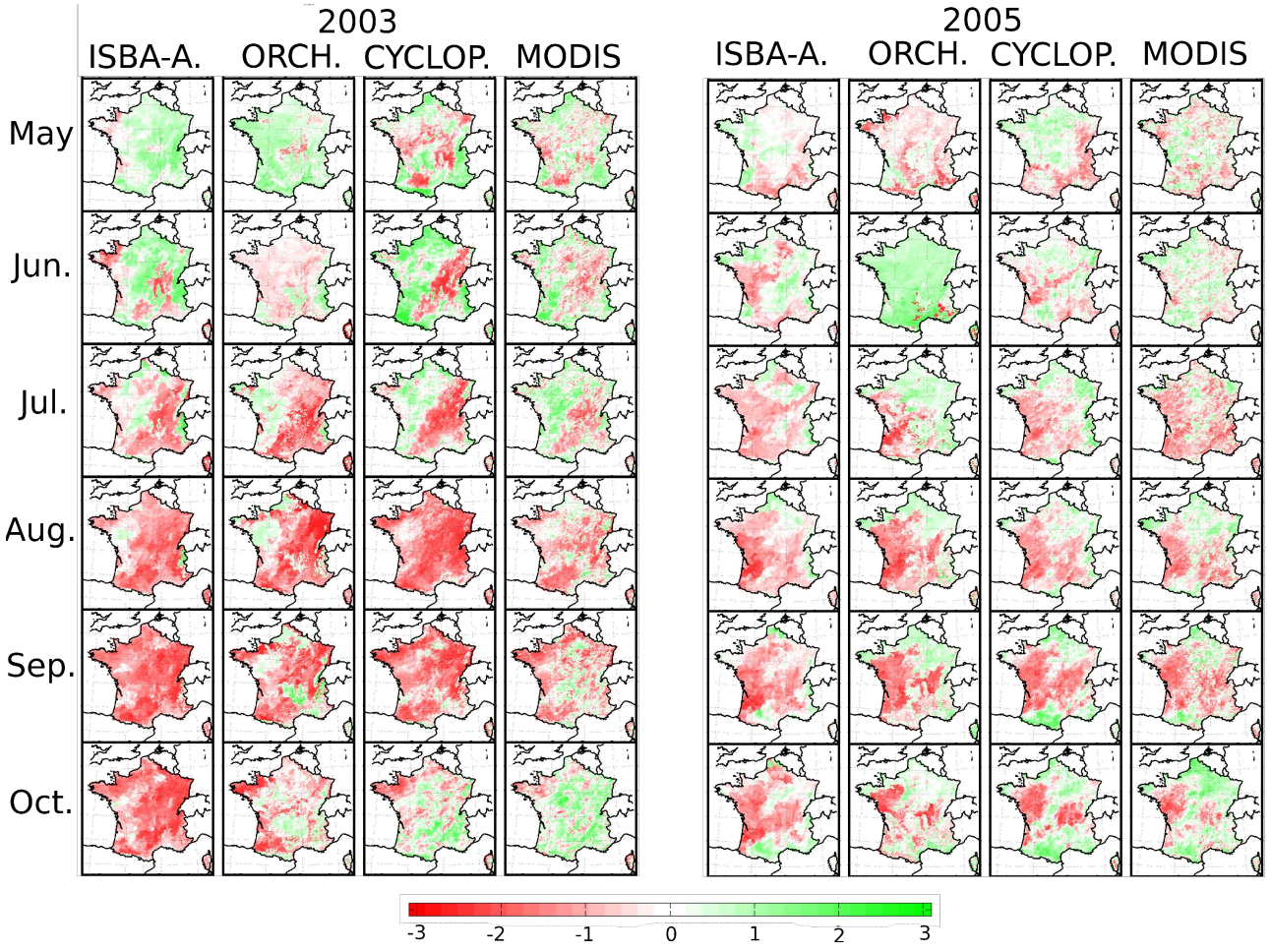

Fig. 5. Scaled LAI anomaly during two years of severe drought (left, 2003 and right, 2005). From left to right: ISBA-A-gs and ORCHIDEE models, CYCLOPES and MODIS remote sensing products. From top to bottom: May to October. Coloured levels correspond to the LAI of the year minus the climatology, then divided by the standard deviation. Units are dimensionless and correspond to standard deviations.

show a positive anomaly in southern France, whereas the models tend to maintain a negative anomaly.

The 2005 drought was less marked than the 2003 drought and affected southwestern France, mainly. Again, a good agreement between the model and the satellite observation can be noticed. In June 2005, the ORCHIDEE scaled LAI anomaly is markedly positive over nearly all the domain, while the other products already display negative anomalies in many regions. It must be noted that the interannual variability of the ORCHIDEE LAI is very small in June, and in this case the scaled anomaly given by Eq. (1) is more likely to display extreme values.

3.4 LAI per vegetation type

The heterogeneity of the landscape is described in the models by a tiling scheme. This means that within a grid point, several model simulations are made (one per PFT), producing their own LAI and flux values, which can be analyzed together with the average grid-cell values. As mentioned previously, in this study, the two models use the same land cover map, and very similar PFT fractions derived from ECOCLIMAP-II.

Figure 6 presents the average LAI seasonal cycle over France per vegetation type. First, it can be noted that each PFT presents a different seasonal cycle and that differences between models are directly linked to the vegetation type. There is a good agreement between ORCHIDEE and ISBA-A-gs for broadleaf forests, and C4 crops. For coniferous forests, the difference in LAI definition (see Sect. 2.4.5) appears clearly: ISBA-A-gs simulates an equivalent photosynthetically active LAI, which has a low value in winter. The summer values are similar for the two models. The main discrepancy concerns C3 crops for which ORCHIDEE simulates a very sharp seasonal cycle with a maximum value in May and a rapid leaf offset in July. ISBA-A-gs simulates a later maximum (in June) and a slower decline of the LAI. Finally, the grassland patch simulations present higher

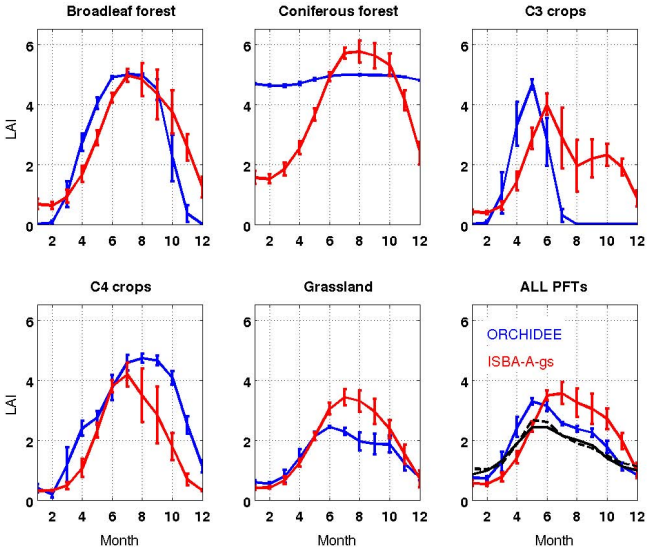

Fig. 6. Average LAI annual cycle simulated by ISBA-A-gs and ORCHIDEE over France for the 1994–2007 period, for each vegetation type. The error bars represent the interannual variability (defined by the standard variation over the period 1994–2007). From left to right, and top to bottom: Broadleaf forests, Coniferous forests, C3 crops, C4 crops, Grasslands, and ALL PFT together. In the latter subfigure, the two black lines represent the average of the two remote sensing products: MODIS (solid), CYCLOPES (dashed), for the 2000–2007 period.

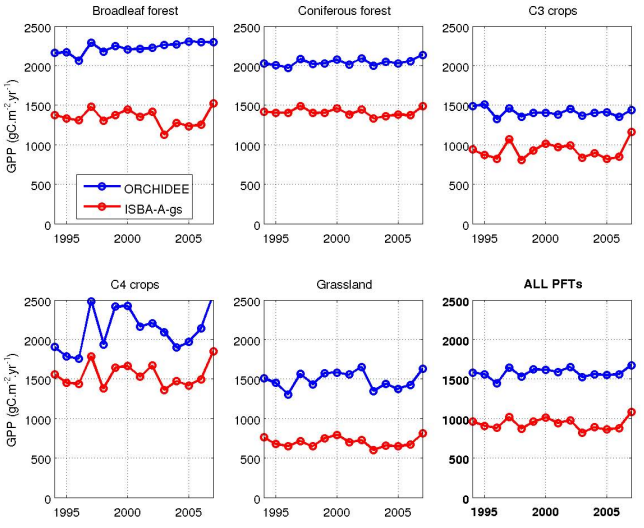

Fig. 7. Interannual variation of the yearly GPP simulated by ISBA-A-gs and ORCHIDEE over France for the 1994–2007 period, for each vegetation type. From left to right, and top to bottom: Broadleaf forests, Coniferous forests, C3 crops, C4 crops, Grasslands, All PFTs.

LAI values for ISBA-A-gs. The average grassland leaf onset simulated by the two models are consistent, with, however, a more intense and longer growth in the ISBA-A-gs simulations. For all the PFTs, the two satellite products (CYCLOPES and MODIS) present a LAI seasonal cycle with a smaller (lower maximum and higher minimum) amplitude than the simulated one.

3.5 Carbon fluxes

The period of analysis of the LAI products (derived from model simulations or from satellite data) was limited by the availability of the remote sensing products to the period 2000–2007. The analysis of carbon and energy fluxes concerns model simulations, only, and was performed over the full length of the simulations (1994–2007, 14 yr). Table 2 presents the monthly values of the energy, water and carbon fluxes averaged over the France domain for the period 1994–2007. The GPP and the Reco carbon fluxes present large differences in amplitude (50 % for the maximum value) and timing (maximum values occur earlier in the ORCHIDEE simulation). The comparison of the fluxes simulated by the two models shows that ORCHIDEE and ISBA-A-gs tend to simulate high and low GPP values, respectively. Less discrepancies are observed for the net ecosystem flux (NEE) and the differences between the two models have the same magnitude as the local differences found by Vetter et al. (2008) using four vegetation models over Europe. Both models use equilibrium assumptions between the plant productivity and Reco. This means that the differences in the magnitude of GPP are equally present in the estimated Reco. As a consequence, this reduces strongly the disagreement on NEE. This modelling choice is supported by in situ measurement that show a good correlation between annual Reco and annual GPP (Janssens et al., 2001; Lasslop et al., 2010). The monthly inter-annual variation is represented in Table 2 by the standard deviation. ORCHIDEE has high variability in spring at the start of the growing season, and very low variability in July. In contrast, the highest variability is observed in summer for ISBA-A-gs. This variability is consistent with the LAI variability seen in Fig. 3.

The differences in simulated fluxes between models are directly linked to the PFT types (Figs. 7 and 8). The PFT impact on the differences in simulated fluxes is more visible on a seasonal basis (Fig. 8), than on an annual basis (Fig. 7). In Fig. 8, it can be observed that the two NEE simulations are more or less consistent, from one PFT to another.

Figure 7 presents the interannual variations in annual GPP year by year, over France.

The two models show similar variations but shifted by about 500 $gCm^{-2}\,yr^{-1}$. A number of years present a higher productivity: 1997, 2000 and 2007. The years 1996, 1998 and 2003 present a lower productivity. The annual GPP varies from one PFT to another with high values for forests and C4 crops; and relatively lower values for C3 crops and grasslands. In this series of annual means, the year 2003 does

Table 2. Average and standard deviation of the main fluxes over France over the 14 yr-period. Maximum monthly values are presented in Bold. The standard deviation represents the inter-annual variability of the spatially averaged fluxes. The annual values (last column) consist of mean yearly accumulated quantities, except for H (annual average).

	Jan.	Feb.	Mar.	Apr.	May	June	July	Aug.	Sept.	Oct.	Nov.	Dec.	Annual
Net ecosystem respiration (NEE) ($gC\,m^{-2}\,month^{-1}$)													
Avg. ORCHIDEE	47.5	38.0	7.2	−70.9	**−132**	−91.6	−10.4	18.0	21.5	43.6	53.6	52.5	−23.2
Avg. ISBA-A-gs	42.0	34.7	25.5	−8.8	−70.9	**−96.0**	−37.6	6.1	3.7	22.5	33.4	41.9	−3.3
std. ORCHIDEE	3.5	3.1	19.8	**20.1**	7.5	18.9	11.3	13.6	4.8	5.7	6.8	5.5	–
std. ISBA-A-gs	3.3	5.1	6.9	14.3	10.8	21.3	**24.6**	19.2	15.7	7.4	6.5	5.4	–
Gross Primary Production (GPP) ($gC\,m^{-2}\,month^{-1}$)													
Avg. ORCHIDEE	16.0	20.2	82.4	205.6	**327.7**	303.3	213.4	163.7	120.6	78.3	31.5	16.9	1579.6
Avg. ISBA-A-gs	7.5	11.4	34.9	78.2	165.2	**203.2**	155.6	108.2	82.0	54.6	23.4	9.5	933.8
std. ORCHIDEE	2.0	5.1	**32.0**	30.9	12.9	20.9	7.9	15.3	11.8	9.9	5.7	2.4	–
std. ISBA-A-gs	2.3	4.0	9.9	18.8	11.6	22.4	**26.2**	22.5	19.0	10.8	5.2	3.0	–
Total Ecosystem Respiration (TER) ($gC\,m^{-2}\,month^{-1}$)													
Avg. ORCHIDEE	63.5	58.2	89.6	134.7	195.6	**211.7**	203.0	181.7	142.1	121.9	85.1	69.3	1556.4
Avg. ISBA-A-gs	49.5	46.1	60.4	69.4	94.4	107.3	**118.0**	114.3	85.8	77.1	56.8	51.4	930.5
std. ORCHIDEE	5.1	7.1	**13.2**	12.2	8.1	9.9	7.3	11.0	10.3	9.8	7.9	6.6	–
std. ISBA-A-gs	5.2	7.0	7.8	8.2	9.5	**12.3**	9.9	11.0	11.2	11.4	7.4	6.2	–
Sensible flux H ($W\,m^{-2}$)													
Avg. ORCHIDEE	0.4	7.7	22.9	35.9	41.6	50.9	**55.5**	45.4	35.0	16.4	7.5	1.3	26.7
Avg. ISBA-A-gs	−2.3	4.1	19.2	31.2	33.0	41.7	**54.0**	44.7	27.8	6.9	−0.4	−3.4	21.4
std. ORCHIDEE	3.9	5.1	6.0	**7.6**	4.7	6.0	4.3	6.4	6.1	5.9	4.3	4.4	–
std. ISBA-A-gs	4.2	5.4	6.2	9.6	4.5	9.2	12.9	**14.0**	7.8	6.0	4.3	4.3	–
Transpiration flux LETR ($mm\,month^{-1}$)													
Avg. ORCHIDEE	0.7	1.5	9.4	25.9	49.3	**60.4**	50.7	37.5	21.7	9.0	2.2	0.7	269.0
Avg. SURFEX	1.1	2.1	8.9	23.1	51.1	**70.6**	53.7	36.9	26.2	14.8	4.5	1.3	294.3
std. ORCHIDEE	0.2	0.5	3.9	7.6	4.6	**9.5**	5.8	3.8	4.4	1.9	0.7	0.2	–
std. SURFEX	0.4	0.9	3.2	8.8	5.8	**10.0**	8.8	8.7	7.6	3.5	1.3	0.5	–

not seem exceptional, and it is not the minimum year for most PFTs. Indeed, the strong reduction of GPP at summertime is partly compensated by higher-than-average GPP values in spring and lower-than-average Reco values in autumn). For forests, however, ISBA-A-gs is more responsive to 2003 than ORCHIDEE. While in ORCHIDEE, the year 1996 seems to produce lower GPP for all the PFTs, 2003 produces the lowest GPP for broadleaf forests in the ISBA-A-gs simulations with a marked decrease in GPP, completely absent from the ORCHIDEE simulation. For grasslands, both models simulate a marked drop in GPP. The two models agree in simulating higher GPP values in 2007. Delpierre et al. (2009) noticed that the spring of 2007 was exceptionally warm and had a positive impact on the start of the growing season. The C4 crops present the highest variability and this is probably due to the uneven distribution of C4 crops in France (4 % of the ecosystems in ECOCLIMAP-II, mainly in southwestern France and in northeastern France).

The LAI is an important driving variable for carbon and water fluxes. However, air temperature and incoming radiation, together with the soil moisture stress, have also a critical influence on the fluxes. This means that despite shifts in the phenological cycle between the two models, the temporal shift of the NEE is much smaller, as can be seen in Fig. 8. There is a good agreement for the broadleaf forests and the grasslands, a slightly more intense seasonal cycle simulated by ISBA-A-gs for the coniferous forests, and a more pronounced disagreement (in timing and in intensity) for the C3 crops. In relation to the LAI cycle, ORCHIDEE has an earlier maximum and a more intense NEE cycle with a strong uptake in May and a strong release of carbon in July and August.

It must be noticed that Figs. 7–8 present average results over a 14-yr period, aggregated at the country level. The interpretation of NEE differences at this scale is not easy. However, a striking feature is that differences in NEE values are much smaller than differences in GPP and LAI values.

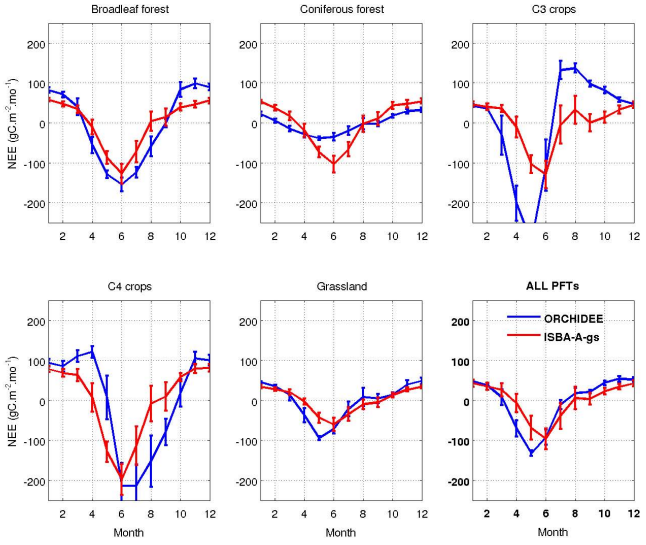

Fig. 8. As in Fig. 6, except for NEE variations. Negative values represents a carbon uptake by the vegetation.

Figure 9 presents additional information about the spatial and seasonal distribution of the average monthly NEE values, on a grid-cell basis, over the whole period (1994–2007). A reasonable spatial agreement is found between the two models and the main patterns are consistent in the two simulations. The main difference is in the magnitude of the fluxes. Consistent with Fig. 8, the land uptake of CO_2 is more marked in ORCHIDEE simulations than for ISBA-A-gs simulations from March to May. While no spatial correlation is observed between the two models in September and in October, excellent spatial correlations are observed at wintertime (December, January, February), with r^2 values higher than 0.55. Fair spatial correlations are observed during the rest of the year (November, and from June to August) with monthly r^2 values ranging from 0.24 to 0.46. The biospheric fluxes obtained by atmospheric inversions (Peters et al., 2010) over Europe at a larger resolution (1 degree) have a smaller magnitude (maximum monthly uptake around $-50\,\mathrm{gCm^{-2}\,month^{-1}}$) than the two models used in this study (maximum values of $-80\,\mathrm{gCm^{-2}\,month^{-1}}$ and $-120\,\mathrm{gCm^{-2}\,month^{-1}}$ for ISBA-A-gs and ORCHIDEE, respectively).

3.6 Water fluxes

Figure 10 presents the average seasonal cycle of plant transpiration. The averaged values over France show a very good agreement between the two models, in terms of seasonal cycle, with a slightly higher maximum value simulated by ISBA-A-gs. However, this overall agreement hides very larges differences between PFTs, as previously noted for the carbon fluxes. There is a reasonable agreement for the coniferous forest PFTs, while much larger values are simulated

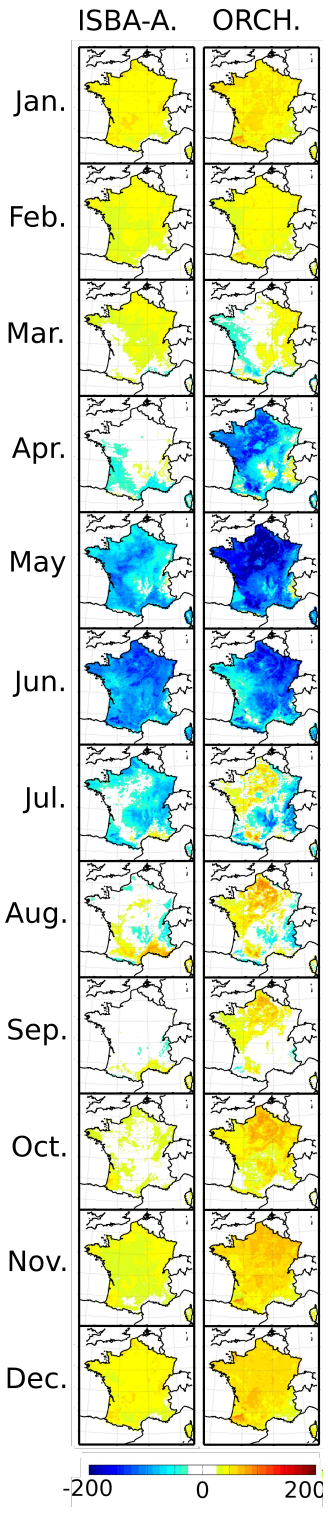

Fig. 9. Average Monthly NEE ($\mathrm{gCm^{-2}\,month^{-1}}$) over France simulated by (left) ISBA-A-gs, (right) ORCHIDEE. Cold and warm colours correspond to an uptake and to a release of carbon by the vegetation, respectively.

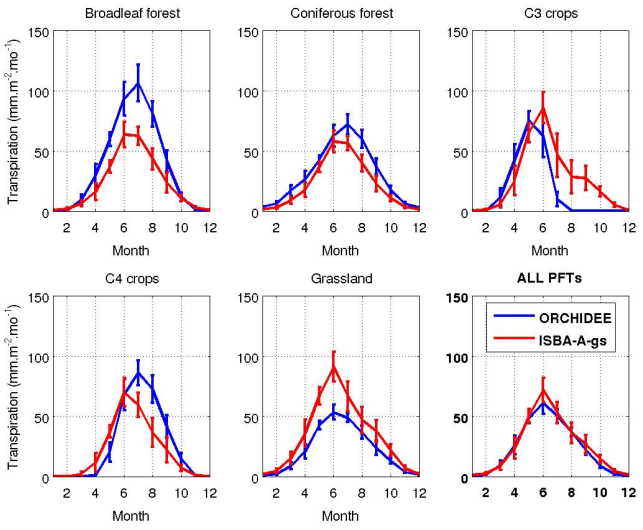

Fig. 10. As in Fig. 6, except for plant transpiration variations.

by ORCHIDEE for the broadleaf forests. Grasslands are the only vegetation type for which ISBA-A-gs simulates higher transpiration rates than ORCHIDEE, throughout the year, which is consistent with the higher LAI values mentioned earlier.

4 Discussion

The comparison of different sources of LAI has shown that the two models present higher maximum LAI values than the remote sensing products. Indeed, the satellite-derived LAI values are affected by a saturation phenomenon at high LAI values, inducing a high uncertainty on yearly maximum LAI values (Garrigues et al., 2008). Moreover, the differences in LAI definition and the contamination by residual noise (atmosphere, clouds) could also partly explain these discrepancies. The use of scaled LAI values permits to better highlight differences in leaf onset and leaf offset.

The plant phenology description is quite different in the two models (see Sect. 2.4.5). While ORCHIDEE uses a phenology model based on an empirical temperature sum model calibrated using satellite data (Botta et al., 2000), ISBA-A-gs simulates a fully photosynthesis-driven LAI. In ISBA-A-gs, the increase of LAI from one day to another is directly related to the amount of photosynthesis achieved during the day. The main advantage of this parameterisation is that it is independent from (calibrated) temperature thresholds, allowing an easier use of the model in coupled mode. A minimum LAI (a parameter set to $0.3\,m^2\,m^{-2}$ for the herbaceous PFTs and the broadleaf forests, set to $1\,m^2\,m^{-2}$ for coniferous forests) allows the start of the growing season. In contrast, in ORCHIDEE, when the date of leaf onset has been reached, depending on temperature and water indicators, reserves are mobilized and the LAI increases quickly to a fixed value. The phenology sub-model of ORCHIDEE permits to simulate the seasonal variability of LAI as observed from space (Fig. 1) better than ISBA-A-gs. The lack of a phenology sub-model in ISBA-A-gs triggers more differences between modelled and satellite-derived seasonal cycles. However, the differences of the two models with the satellite-derived products are less contrasting in terms of interannual variability (Fig. 3) and of scaled anomaly (Fig. 5).

During the growing season, ISBA-A-gs has no predefined limit for the maximum LAI, resulting from the equilibrium of photosynthesis and leaf mortality rates, and strongly influenced by summer droughts. Although this method induces a marked interannual variability, the maximum LAI ranges within physical values. The highest simulated values over France are around $7\,m^2\,m^{-2}$ for forests and crops, and around $5\,m^2\,m^{-2}$ for grasslands. The maximum LAI simulated by the ORCHIDEE model is set by a parameter called LAIMAX. The simulated LAI reaches the maximum value during July for all years and for all PFTs. This means that, in July, the interannual variability of the ORCHIDEE model is almost null (Fig. 3). In ISBA-A-gs, the leaf onset is more sensitive to shortcomings in the model physics (e.g. radiative transfer within the vegetation canopy) and to errors in the atmospheric forcing (Szcypta et al., 2011). On the other hand, the lack of predefined constraints on LAI allows more flexibility in the assimilation of LAI satellite products (Barbu et al., 2011).

Despite differences in the description of the seasonal cycle, both ORCHIDEE and ISBA-A-gs LAI anomalies are consistent with the remote sensing products during extreme events, such as droughts. It must be noticed that in 2003, some disagreements appears in September after the first rainfalls. At the end of the drought, the rains moisten the upper layer of the soil first. Shallow roots are able to quickly use this superficial soil moisture and a plant regrowth may start. In October the remote sensing products show a positive anomaly in southern France, whereas the models tend to maintain a negative anomaly. The soil hydrology in the versions of the models used in this study is represented using a single root zone soil layer. This bucket-type model takes a certain time to recharge, not allowing for a quick restart of the vegetation.

Given that the simulation set-up was designed to minimize discrepancies (the same atmospheric forcing and the same vegetation map were used by the two models), the marked differences in simulated carbon fluxes are caused by differences in the models' physics. The differences between simulations at a regional scale are caused by contrasting parameterizations at the PFT level. Such differences can be partially masked when comparing simulations using different vegetation maps. In this study, they appear more clearly as the same vegetation map is used by the two models. These results show that much research work is needed to reduce modelling uncertainties. However, it must be stressed that the simulation set-up used in this study is particularly demanding for generic models, as global parameters are used over

a relatively small area presenting less contrasting climatic conditions than those encountered in global simulations. As shown in this study, most differences are found in the representation of individual PFTs. Even if the disagreement between models is marked for some ecosystems (i.e. crops), especially for GPP, encouraging similar features are found. For example, while the simulated and satellite-derived LAI seasonal cycle present large differences (Fig. 1), with a shifted cycle for ISBA-A-gs, the various LAI scaled anomalies are remarkably consistent during severe drought events (Fig. 5). The simulated GPP values can be compared with existing estimates over Europe. Schulze et al. (2009) have estimated the natural carbon fluxes over Europe, and they noticed that the average GPP varies little from one PFT to another, with an average value of about 1190 $gCm^2\,yr^{-1}$. The two models used in this study bracket this value (Table 2) with average values over France of 1580 $gCm^2\,yr^{-1}$ and 934 $gCm^2\,yr^{-1}$ for ORCHIDEE and ISBA-A-gs, respectively. In a recent study, Kutsch et al. (2010) provided estimates of GPP for crops over Europe, based on in situ flux observations, ranging between 807 $gCm^2\,yr^{-1}$ and 1624 $gCm^2\,yr^{-1}$, with an average value of 1246 $gCm^2\,yr^{-1}$. The models give values for C3 crops similar to the extremes of this distribution: ORCHIDEE simulates values around 1400 $gCm^2\,yr^{-1}$ while ISBA-A-gs values are around 900 $gCm^2\,yr^{-1}$. It must be noted that Kustch et al. (2010) mention that the sampling uncertainty due to the small number of sites is bigger than the uncertainty of the measurements.

Overall, the two models agree better on the magnitude of the sensible heat flux and of the transpiration flux (Table 2), than on the magnitude of the carbon fluxes, but significant differences are observed for individual PFTs (Fig. 10).

5 Conclusions

Four different LAI products were compared over France, either simulated or derived from satellite observations. These products show important differences in magnitude, timing, and seasonal patterns. For the models, an important part of the differences can be explained by (i) the choice of a weak or a strong constraint on the phonological cycle, (ii) the lack of a detailed representation of the sub-grid farming practices such as crop rotation and winter vs. summer crops. Regarding the latter issue, the two model versions used in this study do not include a representation of farming practices per se. This may explain why most LAI and NEE differences between the two models are observed for crop PFTs (Figs. 6–8). Remote sensing products may provide very useful information on the actual farming practices. This information can be included in the model by using data assimilation techniques and LAI remote sensing information (Albergel et al., 2010a; Jarlan et al., 2008; Barbu et al., 2011). However, the use of data assimilation techniques raises the problem of the remote sensing product accuracy. As shown in this study, as in past studies (Ganguly et al., 2008, Garrigues et al., 2008, Weiss et al., 2007), remote sensing LAI products generally agree in representing the LAI temporal variation, while discrepancies are observed in terms of LAI level (mainly due to saturation effects). Past studies showed that remote sensing products agree better for FAPAR estimates than for LAI (Seixas et al., 2009; Weiss et al., 2007; McCallum et al., 2010). LSMs could be adapted to assimilate this variable. The analysis of the carbon and water fluxes shows smaller differences in seasonal cycle between models than for LAI. It is shown that an overall agreement at the grid-cell level can mask marked flux differences at the sub-grid ecosystem level.

Finally this study points out the importance of (i) the managed ecosystems and the need to work towards a more detailed representation of agricultural practices (e.g. irrigated crops in ISBA-A-gs; Calvet et al., 2008, agricultural modules in ORCHIDEE-STICS; Smith et al., 2010, and JULES-SUCROS; van der Hoof et al., 2010), (ii) a combined evaluation of carbon, water, and energy fluxes, (iii) using a common forcing and input land cover maps to perform model benchmarking, as a model agreement at the country level can mask strong differences at the ecosystem level. Using a common forcing and input land cover maps permits avoiding discrepancies in the simulated vegetation biomass that would lead to wrong conclusions regarding the intrinsic model performances. However, benchmarking in not only a matter of intercomparison methodology. Relevant data sets, as accurate as possible, have to be used. For example, Calvet et al. (2012) have tested the use of agricultural yield statistics to compare several parameter configurations of the ISBA-A-gs model. They show that, even if ISBA-A-gs does not simulate specific processes related to agricultural practices, the agricultural statistics have potential to evaluate the impact of key model parameters, in particular those related to the plant response to drought. Finally, new LAI and FAPAR products (BIOPAR-V1) are being prepared by the GEOLAND-2 project. As they will be available in near-real-time, they will permit a continuous quality control of model-based monitoring systems. Ultimately, they could be assimilated in land surface models, as shown by Barbu et al. (2011).

Acknowledgements. This work is a contribution to the GEOLAND2 project, co-funded by the European Commission within the GMES initiative in FP7, to the GHG-Europe FP7 project, and to the CarboFrance project “Impact des extrêmes climatiques sur les flux de carbone” (GICC, French project).

Edited by: D. F. Prieto

The publication of this article is financed by CNRS-INSU.

References

Albergel, C., Calvet, J.-C., Mahfouf, J.-F., Rüdiger, C., Barbu, A. L., Lafont, S., Roujean, J.-L., Walker, J. P., Crapeau, M., and Wigneron, J.-P.: Monitoring of water and carbon fluxes using a land data assimilation system: a case study for southwestern France, Hydrol. Earth Syst. Sci., 14, 1109–1124, doi:10.5194/hess-14-1109-2010, 2010a.

Albergel, C., Calvet, J.-C., Gibelin, A.-L., Lafont, S., Roujean, J.-L., Berne, C., Traullé, O., and Fritz, N.: Observed and modelled ecosystem respiration and gross primary production of a grassland in southwestern France, Biogeosciences, 7, 1657–1668, doi:10.5194/bg-7-1657-2010, 2010b.

Baldocchi, D. D.: Turner review No. 15, "Breathing" of the terrestrial biosphere: lessons learned from a global network of carbon dioxide flux measurement systems, Aust. J. Bot., 56, 1–26, doi:10.1071/BT07151, 2008.

Ball, J., Woodrow, T., and Berry, J.: A model predicting stomatal conductance and its contribution to the control of photosynthesis under different environmental conditions, Prog. Photosynthesis, 4, 221–224, 1987.

Barbu, A. L., Calvet, J.-C., Mahfouf, J.-F., Albergel, C., and Lafont, S.: Assimilation of Soil Wetness Index and Leaf Area Index into the ISBA-A-gs land surface model: grassland case study, Biogeosciences, 8, 1971–1986, doi:10.5194/bg-8-1971-2011, 2011.

Baret, F., Hagolle, O., Geiger, B., Bicheron, P., Miras, B., Huc, M., Berthelot, B., Niño, F., Weiss, M., Samain, O., Roujean, J.-L., and Leroy, M.: LAI, fAPAR and fCover CYCLOPES global products derived from VEGETATION, Part 1: Principles of the algorithm, Remote Sens. Environ., 110, 275–286, 2007.

Botta, A., Viovy, N., Ciais, P., and Friedlingstein, P.: A global prognostic scheme of leaf onset using satellite data, Glob. Change Biol., 6, 709–726, 2000.

Brut, A., Ru¨diger, C., Lafont, S., Roujean, J.-L., Calvet, J.-C., Jarlan, L., Gibelin, A.-L., Albergel, C., Le Moigne, P., Soussana, J.-F., Klumpp, K., Guyon, D., Wigneron, J.-P., and Ceschia, E.: Modelling LAI at a regional scale with ISBA-A-gs: comparison with satellite-derived LAI over southwestern France, Biogeosciences, 6, 1389–1404, doi:10.5194/bg-6-1389-2009, 2009.

Calvet, J.-C.: Investigating soil and atmospheric plant water stress using physiological and micrometeorological data sets, Agr. Forest Meteorol., 103, 229–247, 2000.

Calvet, J.-C. and Soussana, J.-F.: Modelling CO_2-enrichment effects using an interactive vegetation SVAT scheme, Agr. Forest Meteorol., 108, 129–152, 2001.

Calvet, J.-C., Noilhan, J., Roujean, J.-L., Bessemoulin, P., Cabelguenne, M., Olioso, A., and Wigneron, J.-P.: An interactive vegetation SVAT model tested against data from six contrasting sites, Agr. Forest Meteorol., 92, 73–95, 1998.

Calvet, J.-C., Rivalland, V., Picon-Cochard, C., and Guehl, J.-M.: Modelling forest transpiration and CO_2 fluxes – response to soil moisture stress, Agr. Forest Meteorol., 124(3–4), 143–156, doi:10.1016/j.agrformet.2004.01.007, 2004.

Calvet, J.-C., Gibelin, A.-L., Roujean, J.-L., Martin, E., Le Moigne, P., Douville, H., and Noilhan, J.: Past and future scenarios of the effect of carbon dioxide on plant growth and transpiration for three vegetation types of southwestern France, Atmos. Chem. Phys., 8, 397–406, doi:10.5194/acp-8-397-2008, 2008.

Calvet, J.-C., Lafont, S., Cloppet, E., Souverain, F., Badeau, V., and Le Bas, C.: Use of agricultural statistics to verify the interannual variability in land surface models: a case study over France with ISBA-A-gs, Geosci. Model Dev., 5, 37–54, doi:10.5194/gmd-5-37-2012, 2012.

Chen, J. M., Menges, C. H., and Leblanc, S. G.: Global mapping of foliage clumping index using multi-angular satellite data, Remote Sens. Environ., 97(4), 447–457, 2005.

Collatz, G. J., Ribas-Carbo, M., and Berry, J. A.: Coupled photosynthesis-stomatal conductance model for leaves of C4 plants, Aust. J. Plant Physiol., 19, 519–538, 1992.

Courtier, P., Freydier, C., Geleyn, J.-F., Rabier, F., and Rochas, M.: The Arpège project at Météo-France, Proc. ECMWF Seminar on Numerical Methods in Atmospheric Models, ECMWF, Reading, UK, 2, 193–232, 1991.

de Rosnay, P. and Polcher, J.: Modelling root water uptake in a complex land surface scheme coupled to a GCM, Hydrol. Earth Syst. Sci., 2, 239–255, doi:10.5194/hess-2-239-1998, 1998.

Delpierre, N., Soudani, K., François, C., Köstner, B., Pontailler, J.-Y., Nikinmaa, E., Misson, L., Aubinet, M., Bernhofer, C., Granier, A., Grünwald, T., Heinesch, B., Longdoz, B., Ourcival, J.-M., Rambal, S., Vesala, T., and Dufrêne, E.: Exceptional carbon uptake in European forests during the warm spring of 2007: a data-model analysis, Glob. Change Biol., 15(6), 1455–1474, doi:10.1111/j.1365-2486.2008.01835.x, 2009.

Demarty, J., Chevallier, F., Friend, A. D., Viovy, N., Piao, S., and Ciais, P.: Assimilation of global MODIS leaf area index retrievals within a terrestrial biosphere model, Geophys. Res. Lett., 34, L15402, doi:10.1029/2007GL030014, 2007.

Dickinson, R. E., Henderson-sellers, A., Rosenzweig, C., and Sellers, P. J.: Evapotranspiration models with canopy resistance for use in climate models, a review, Agr. Forest Meteorol., 54, 373–388, doi:10.1016/0168-1923(91)90014-H, 1991.

Durand, Y., Brun, E., Merindol, L., Guyomarc'h, G., Lesaffre, B., and Martin, E.: A meteorological estimation of relevant parameters for snow models, Ann. Glaciol., 18, 65–71, 1993.

Durand, Y., Giraud, G., Brun, E., Merindol, L., and Martin, E.: A computer-based system simulating snow-pack structures as a tool for regional avalanche forecasting, Ann. Glaciol., 45, 469–484, 1999.

Farquhar, G., von Caemmerer, S., and Berry, J.: A biochemical model of photosynthesis CO_2 fixation in leaves of C3 species, Planta, 149, 78–90, 1980.

Faroux, S., Roujean, J.-L., Kaptué, A., and Masson, V. : La base de données de paramètres de surface ECOCLIMAP-II sur l'Europe, Note de centre du Groupe de Météorologie à Moyenne Echelle, 86, Météo-France, CNRM, Toulouse, France, 120 pp., 2009.

Foley, J. A., Prentice, I. C., Ramunkutty, N., Levis, S., Pollard, D., Sitch, S., and Haxeltine, A.: An integrated biosphere model of land surface processes, terrestrial carbon balance en vegetation dynamics, Global Biogeochem. Cy., 10, 603–628, 1996.

Friedl, M. A., McIver, D. K., Hodges, J. C. F., Zhang, X. Y., Muchoney, D., Strahler, A. H., Woodcock, C. E., Gopal, S., Schneider, A., Cooper, A., Baccini, A., Gao, F., and Schaaf, C. B.: Global land cover mapping from MODIS: algorithms and early results, Remote Sens. Envir., 83, 287–302, doi:10.1016/S0034-4257(02)00078-0, 2002.

Ganguly, S., Samanta, A., Schull, M. A., Shabanov, N. V., Milesi, C., Nemani, R. R., Knyazikhin, Y., and Myneni, R. B.: Generating vegetation leaf area index Earth system data record from multiple sensors, Part 2: Implementation, analysis and valida-

tion, Remote Sens. Environ., 112, 4318–4332, 2008.

Garratt, J. R.: Sensitivity of Climate Simulations to Land-Surface and Atmospheric Boundary-Layer Treatments – A Review, J. Climate, 6, 419–448, 1993.

Garrigues, S., Lacaze, R., Baret, F., Morisette, J. T., Weiss, M., Nickeson, J. E., Fernandes, R., Plummer, S., Shabanov, N. V., Myneni, R. B., Knyazikhin, Y., and Wang, W.: Validation and intercomparison of global Leaf Area Index products derived from remote sensing data, J. Geophys. Res., 113, G02028, doi:10.1029/2007JG000635, 2008.

Gibelin, A., Calvet, J.-C., Roujean, J.-L., Jarlan, L., and Los, S. O.: Ability of the land surface model ISBA-A-gs to simulate leaf area index at the global scale: Comparison with satellites products, J. Geophys. Res., 111, 1–16, 2006.

Gibelin, A.-L., Calvet, J.-C., and Viovy, N.: Modelling energy and CO_2 fluxes with an interactive vegetation land surface model evaluation at high and middle latitudes, Agr. Forest Meteorol., 148, 1611–1628, 2008.

Goudriaan, J., van Laar, H.H., van Keulen, H., and Louwerse, W.: Photosynthesis, CO_2 and plant production,in: Wheat growth and modelling, NATO ASI Series, edited by: Day, W. and Atkin, R. K., Plenum Press, New York, Series A, 86, 107–122, 1985.

Jacobs, C. M. J.: Direct impact of CO_2 enrichment on regional transpiration, Ph. D. Thesis, Agricultural University, Wageningen, 1994.

Jacobs, C. M. J., Van den Hurk, B. J. J. M., and De Bruin, H. A. R.: Stomatal behaviour and photosynthetic rate of unstressed grapevines in semi-arid conditions, Agr. Forest Meteorol., 80, 111–134, 1996.

Jarlan, L., Balsamo, G., Lafont, S., Beljaars, A., Calvet, J.-C., and Mougin, E.: Analysis of leaf area index in the ECMWF land surface model and impact on latent heat and carbon fluxes: application to West Africa, J. Geophys. Res., 113, 1–22, doi:10.1029/2007JD009370, 2008.

Janssens, I. A., Lankreijer, H., Matteucci, G., Kowalski, A. S., Buchmann, N., Epron, D., Pilegaard, K., Kutsch, W., Longdoz, B., Grunwald, T., Montagnani, L., Dore, S., Rebmann, C., Moors, E. J., Grelle, A., Rannik, Ü., Morgenstern, K., Olchev, S., Clement, R., Gudmundsson, J., Minerbi, S., Berbigier, P., Ibrom, A., Moncrieff, J., Aubinet, M., Bernhofer, C., Jensen, N. O., Vesala, T., Granier, A., Schulze, E. D., Lindroth, A., Dolman, A.J., Jarvis, P.G., Ceulemans, R., and Valentini, R.: Productivity overshadows temperature in determining soil and ecosystem respiration across European forests, Glob. Change Biol., 7(3), 269–278, doi:10.1046/j.1365-2486.2001.00412.x, 2001.

Jung, M., Le Maire, G., Zaehle, S., Luyssaert, S., Vetter, M., Churkina, G., Ciais, P., Viovy, N., and Reichstein, M.: Assessing the ability of three land ecosystem models to simulate gross carbon uptake of forests from boreal to Mediterranean climate in Europe, Biogeosciences, 4, 647–656, doi:10.5194/bg-4-647-2007, 2007.

Knyazikhin, Y., Martonchik, J. V., Myneni, R. B., Diner, D. J., and Running, S. W.: Synergistic algorithm for estimating vegetation canopy leaf area index and fraction of absorbed photosynthetically active radiation from MODIS and MISR data, J. Geophys. Res., 103, 32257-32275, doi:10.1029/98JD02462, 1998.

Krinner, G., Viovy, N., de Noblet-Ducoudré, N., Ogée, J., Polcher, J., Friedlingstein, P., Ciais, P., Sitch, S., and Prentice, I.: A dynamic global vegetation model for studies of the coupled atmosphere-biosphere system, Glob. Biogeochem. Cy., 19, GB1015, doi:10.1029/2003GB002199, 2005.

Kutsch, W. L., Aubinet, M., Buchmann, N., Smith, P., Osborne, B., Eugster, W., Wattenbach, M., Schrumpf, M., Schulze, E.-D., and Tomelleri, E.: The net biome production of full crop rotations in Europe, Agriculture, Ecosyst. Environ., 139, 336–345, doi:10.1016/j.agee.2010.07.016, 2010.

Lasslop, G., Reichstein, M., Papale, D., Richardson, A. D., Arneth, A., Barr, A. G., Stoy, P., and Wohlfahrt, G.: Separation of net ecosystem exchange into assimilation and respiration using a light response curve approach: critical issues and global evaluation, Glob. Change Biol., 16(1), 187–208, doi:10.1111/j.1365-2486.2009.02041.x, 2010.

Le Maire, G., Delpierre, N., Jung, M., Ciais, P., Reichstein, M., Viovy, N., Granier, A., Ibrom, A., Kolari, P., Longdoz, B., Moors, E. J., Pilegaard, K., Rambal, S., Richardson, A. D., and Vesala, T.: Detecting the critical periods that underpin interannual fluctuations in the carbon balance of European forests, J. Geophys. Res., 115, G00H03, doi:10.1029/2009JG001244, 2010.

Le Moigne, P., Boone, A., Calvet, J.-C., Decharme, B., Faroux, S., Gibelin, A.-L., Lebeaupin, C., Mahfouf, J.-F., Martin, E., Masson, V., Mironov, D., Noilhan, J., Tulet, P., and Van Den Hurk, B.: SURFEX scientific documentation. Note de centre du Groupe de Météorologie à Moyenne Echelle, 87, Météo-France, CNRM, Toulouse, France, 211 pp., available at: http://www.cnrm.meteo.fr/surfex/, last access: July 2011, 2009.

McCallum, I., Wagner, W., Schmullius, C., Shvidenko, A., Obersteiner, M., Fritz, S., and Nilsson, S.: Comparison of four global FAPAR datasets over Northern Eurasia for the year 2000., Remote Sens. Environ., 114, 941–949, 2010.

Maignan, F., Bréon, F.-M., Chevallier, F., Viovy, N., Ciais, P., Garrec, C., Trules, J., and Mancip, M.: Evaluation of a Global Vegetation Model using time series of satellite vegetation indices, Geosci. Model Dev., 4, 1103-1114, doi:10.5194/gmd-4-1103-2011, 2011.

Masson, V., Champeaux, J.-L., Chauvin, F., Meriguet, C., and Lacaze, R.: A global database of land surface parameters at 1-km resolution in meteorological and climate models, J. Climate, 16, 1261–1282, 2003.

McMurtrie, R. E, Rook, D. A., and Kelliher, F.: Modelling the yield of pinus radiata on a site limited by water and nitrogen, Forest Ecol. Manag., 30, 381–413, 1990.

Morales, P., Sykes, M. T., Prentice, I. C., Smith, P., Smith, B., Bugmann, H., Zierl, B., Friedlingstein, P., Viovy, N., Sabate, S., Sanchez, A., Pla, E., Gracia, C., Sitch, S., Arneth, A., and Ogée, J.: Comparing and evaluating process-based ecosystem model predictions of carbon and water fluxes in major European forest biomes, Glob. Change Biol., 11, 2211–2233, doi:10.1111/j.1365-2486.2005.01036.x, 2005.

Peters, W., Krol, M. C., Van Der Werf, G. R., Houweling, S., Jones, C. D., Hughes, J., Schaefer, K., Masarie, K. A., Jacobson, A. R., Miller, J. B., Cho, C. H., Ramonet, M., Schmidt, M., Ciattaglia, L., Apadula, F., Heltai, D., Meinhardt, F., Di Sarra, A. G., Piacentino, S., Sferlazzo, D., Aalto, T., Hatakka, J., Ström, J., Haszpra, L., Meijer, H. A. J., Van Der Laan, S., Neubert, R. E. M., Jordan, A., Rodó, X., Morgui, J.-A., Vermeulen, A. T., Popa, E., Rozanski, K., Rozanski, K., Zimnoch, M., Manning, A. C., Leuenberger, M., Uglietti, C., Dolman, A.J., Ciais, P., Heimann,

M., and Tans, P. P.: Seven years of recent European net terrestrial carbon dioxide exchange constrained by atmospheric observations, Glob. Change Biol., 16, 1317–1337, doi:10.1111/j.1365-2486.2009.02078.x, 2010.

Pitman, A. J.: The evolution of, and revolution in, land surface schemes designed for climate models, Int. J. Climatol., 23, 479–510, 2003.

Quintana-Segui, P., Le Moigne, P., Durand, Y., Martin, E., Habets, F., Baillon, M., Canellas, C., Franchistéguy, L., and Morel, S.: Analysis of near surface atmospheric variables: validation of the SAFRAN analysis over France, J. Appl. Meteorol. Clim., 47, 92–107, 2008.

Ritter, B. and Geleyn, J.-F.: A comprehensive radiation scheme of numerical weather prediction with potential application to climate simulations, Mon. Weather Rev., 120, 303–325, 1992.

Sabater, J. M., Rüdiger, C., Calvet, J.-C., Fritz, N., Jarlan, L., and Kerr, Y.: Joint assimilation of surface soil moisture and LAI observations into land surface model, Agric. For. Meteorol., 148, 1362–1373, doi:10.1016/j.agrformet.2008.04.003, 2008.

Schulze, E.-D., Luyssaert, S., Ciais, P., Freibauer, A., Janssens, I. A., Soussana, J. F., Smith, P., Grace, J., Levin, I., Thiruchittampalam, B., Heimann, M., Dolman, A. J., Valentini, R., Bousquet, P., Peylin, P., Peters, W., R¨odenbeck, C., Etiope, G., Vuichard, N., Wattenbach, M., Nabuurs, G. J., Poussi, Z., Nieschulze, J., and Gash, J. H.: Importance of methane and nitrous oxide for Europe's terrestrial greenhouse-gas balance, Nat. Geosci., 2, 842–850, doi:10.1038/ngeo686, 2009.

Seixas, J., Carvalhais, N., Nunes, C., and Benali, A.: Comparative analysis of MODIS-FAPAR and MERIS-MGVI datasets: potential impacts on ecosystem modelling, Remote Sens. Environ., 113, 2547–2559, 2009.

Sellers, P. J., Randall, D. A., Collatz, G. J., Berry, J. A., Field, C. B., Dazlich, D. A., Zhang, C., Collelo, G. D., and Bounoua, L.: A revised land surface parameterization (SiB2) for atmospheric GCMs, Pt. I : Model Formulation, J. Climate, 9, 676–705, 1996.

Seneviratne, S. I., Lüthi, D., Litschi, M., and Schär, C.: Land-atmosphere coupling and climate change in Europe., Nature, 443, 205–209, doi:10.1038/nature05095, 2006.

Sitch, S., Smith, B., Prentice, I. C., Arneth, A., Bondeau, A., Cramer,W., Kaplan, J. O., Levis, S., Lucht, W., Sykes, M. T., Thonicke, K., and Venevsky, S.: Evaluation of ecosystem dynamics, plant geography and terrestrial carbon cycling in the LPJ dynamic vegetation model, Glob. Change Biol., 9, 161–185, 2003.

Smith, P. C., De Noblet-Ducoudré, N., Ciais, P., Peylin, P., Viovy, N., Meurdesoif, Y., and Bondeau, A.: European-wide simulations of croplands using an improved terrestrial biosphere model: phenology and productivity, J. Geophys. Res., 115, G01014, doi:10.1029/2008JG000800, 2010.

Szczypta, C., Calvet, J.-C., Albergel, C., Balsamo, G., Boussetta, S., Carrer, D., Lafont, S., and Meurey, C.: Verification of the new ECMWF ERA-Interim reanalysis over France, Hydrol. Earth Syst. Sci., 15, 647–666, doi:10.5194/hess-15-647-2011, 2011.

Van den Hoof, C., Hanert, E., and Vidale, P. L.: Simulating dynamic crop growth with an adapted land surface model – JULES-SUCROS: Model development and validation, Agr. Forest Meteorol., 151, 137–153, doi:10.1016/j.agrformet.2010.09.011, 2010.

Verger, A., Camacho, F., Garcia-Haro, F., and Melia, J.: Prototyping of Land-SAF leaf area index algorithm with VEGETATION and MODIS data over Europe, Remote Sens. Environ., 113, 2285–2297, 2009.

Verhoef, W.: Light scattering by leaf layers with application to canopy reflectance modeling: the SAIL model, Remote Sens. Environ., 16, 125–141, 1984.

Vetter, M., Churkina, G., Jung, M., Reichstein, M., Zaehle, S., Bondeau, A., Chen, Y., Ciais, P., Feser, F., Freibauer, A., Geyer, R., Jones, C., Papale, D., Tenhunen, J., Tomelleri, E., Trusilova, K., Viovy, N., and Heimann, M.: Analyzing the causes and spatial pattern of the European 2003 carbon flux anomaly using seven models, Biogeosciences, 5, 561–583, doi:10.5194/bg-5-561-2008, 2008.

Vidal, J.-P., Martin, E., Franchistéguy, L., Baillon, M., and Soubeyroux, J.-M.: A 50-year high-resolution atmospheric reanalysis over France with the Safran system, Int. J. Climatol., 30, 1627–1644, doi:10.1002/joc.2003, 2010.

Viovy, N.: PILPS carbon first experiment, available at: http://pilpsc1.lsce.ipsl.fr/, last access: January 2012, 2003.

Vuichard, N., Soussana, J.-F., Ciais, P., Viovy, N., Ammann, C., Calanca, P., Clifton-Brown, J., Fuhrer, J., Jones, M., and Martin, C.: Estimating the greenhouse gas fluxes of European grasslands with a process-based model: 1. Model evaluation from in situ measurements, Global Biogeochem. Cy., 21, GB1004, doi:10.1029/2005GB002611, 2007.

Weiss, M., Baret, F., Garrigues, S., and Lacaze, R.: LAI and fAPAR CYCLOPES global products derived from VEGETATION, Part 2: validation and comparison with MODIS collection 4 products, Remote Sens. Environ., 110, 317–331, doi:10.1016/j.rse.2007.03.001, 2007.

Zhao, Y., Ciais, P., Peylin, P., Viovy, N., Longdoz, B., Bonnefond, J. M., Rambal, S., Klumpp, K., Olioso, A., Cellier, P., Maignan, F., Eglin, T., and Calvet, J.C.: How errors on meteorological variables impact simulated ecosystem fluxes: a case study for six French sites, Biogeosciences Discuss., 8, 2467–2522, doi:10.5194/bgd-8-2467-2011, 2011.